

Dynamical changes in neurons during seizures determine tonic to clonic shift

Bryce Beverlin II · James Kakalios · Duane Nykamp ·
Theoden Ivan Netoff

Received: 15 April 2011 / Revised: 30 October 2011 / Accepted: 3 November 2011 / Published online: 30 November 2011
© Springer Science+Business Media, LLC 2011

Abstract A tonic-clonic seizure transitions from high frequency asynchronous activity to low frequency coherent oscillations, yet the mechanism of transition remains unknown. We propose a shift in network synchrony due to changes in cellular response. Here we use phase-response curves (PRC) from Morris-Lecar (M-L) model neurons with synaptic depression and gradually decrease input current to cells within a network simulation. This method effectively decreases firing rates resulting in a shift to greater network synchrony illustrating a possible mechanism of the transition phenomenon. PRCs are measured from the M-L conductance based model cell with a range of input currents within the limit cycle. A large network of 3000 excitatory neurons is simulated with a network topology generated from second-order statistics which allows a range of population synchrony. The population synchrony of the oscillating cells is measured with the Kuramoto order parameter, which reveals a transition from tonic to clonic phase exhibited by our model

network. The cellular response shift mechanism for the tonic-clonic seizure transition reproduces the population behavior closely when compared to EEG data.

Keywords Seizure model · PRC · Tonic clonic · Synchrony

1 Introduction

1.1 Tonic-clonic seizure

At the onset of seizures, high frequency low amplitude oscillations are observed in EEG accompanied by tonic flexion of the axial musculature (Bragin et al. 2010; Fisch and Olejniczak 2006). This finding has since been corroborated during the seizure using intracranial EEG recordings (Schindler et al. 2007b) and MEG (Garcia Dominguez et al. 2005; Perez Velazquez et al. 2007). The tonic phase slowly transitions to the clonic phase passing through an “intermediate vibratory period” of 8 Hz oscillations and ending in regular bursting at 4 Hz (Gastaut and Broughton 1972). A stimulus that increases synchrony during a seizure has been shown to truncate the seizure (Schindler et al. 2007a). It has also been shown that firing rates of neurons *in vivo* decrease over the course of the tonic-clonic seizure (Ward 1961), arguably starting during the pre-ictal period progressing to the onset of the seizure, in most cases ending in a form of auto-termination.

In grand-mal seizures there is a tonic phase, where the patient tenses the muscles accompanied by high frequency low amplitude neural activity, followed by a transition to clonic phase, where convulsive contractions of the muscles are accompanied by low frequency large amplitude EEG activity (Quian Quiroga et al. 1997).

Action Editor: David Terman

B. Beverlin II · J. Kakalios
Department of Physics, University of Minnesota,
Minneapolis, MN, USA

D. Nykamp
Department of Mathematics, University of Minnesota,
Minneapolis, MN, USA

T. I. Netoff (✉)
Department of Biomedical Engineering, University of Minnesota,
Minneapolis, MN, USA
e-mail: tnetoff@umn.edu

Synchrony in epilepsy, as measured by the precise timing of the synaptic inputs of two cells in close proximity to each other, decreases during the tonic phase of the seizure and then increases during the clonic phase (Netoff and Schiff 2002). It is evident from EEG data that population amplitude and coherence appears to be greater in the clonic phase as shown in Fig. 1 (data from (Quiroga et al. 1997)).

At the onset of the seizure the neurons are firing at very high rates and each cell is receiving large amounts of input current. As the firing rate slows down, the network transitions to a synchronous high amplitude clonic phase of seizure. We hypothesize that the transition from tonic to clonic phases is caused by a phase response shift in the neurons due to a decrease in firing rates within the network, leading to a shift in synchrony. We demonstrate how the transition occurs in a network of model neurons and explain the mechanisms using pulse-coupled oscillator theory. There are several ways in which network synchrony may change *in vivo*, including the reintroduction of activity from the inhibitory population (provided they have entered depolarization block at the seizure onset) Ziburkus et al. 2006, synaptic depression, and vesicle depletion. In our model, the change in firing rate is produced by including synaptic depression and a gradually decreasing input current to the model neurons.

1.2 PRCs

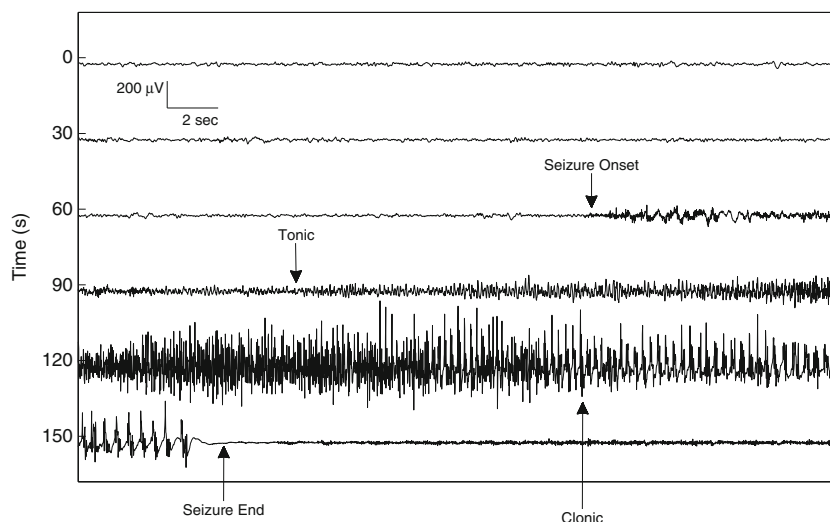
To determine how a network of neurons will synchronize, we need to know the neural network connectivity

and the resetting of the neurons from synaptic input. Because the dynamics of neurons and synapses are rather complicated, analyzing a network of model neurons quickly becomes analytically intractable. An alternative approach is to reduce the complexity of the neuron to a simplistic model. One approach is to model the neuron as a simple input–output function that adjusts the neuron’s next spike-time given the phase of synaptic input; this approach is known as a phase-response curve (PRC) model (Winfree 2001; Ermentrout and Kopell 1998). PRC theory has been used to study synchrony in networks of heart cells (Glass and Mackey 1988), fireflies (Winfree 2001) and neurons (Kopell and Ermentrout 2002; Hoppensteadt and Izhikevich 1997; Izhikevich 2007; Brown et al. 2004). This analytical approach can be used to understand how oscillator networks synchronize (Hansel et al. 1995; Neltner et al. 2000; Ermentrout and Kleinfeld 2001; Mancilla et al. 2007). Given the caveat that neurons fire periodically PRC theory can predict whether a network of neurons can synchronize. The neuron’s measured PRC is dependent on the ionic channel dynamics of the neuron and the synaptic stimulus waveform (Ermentrout et al. 2011). As a neuron’s firing rate changes, the resulting PRC changes. We hypothesize that during a seizure the firing rate of the neurons change, which changes the rate of convergence to the synchronous state.

1.3 Connecting PRC with network synchrony

It has been previously shown that synchrony in networks depends on the firing rate of the neurons

Fig. 1 Tonic-clonic seizure. EEG data of a tonic-clonic seizure recorded using a scalp right central (C4) electrode (linked earlobe reference). Seizure onset is marked by increased activity leading to a tonic phase marked by incoherent increased firing of the neuronal population. High frequency activity continues throughout the tonic phase until coherent oscillations are observed, demarcated by the clonic phase. The seizure terminates when neuronal activity returns to initial baseline levels. Data from Quiroga et al. 1997



(Lewis and Rinzel 2003). We have found that when the network firing rate is very high, network synchrony is less stable compared to when firing rate is slow and the synchronous network activity becomes stable enough to allow synchrony. We propose that as the firing rate slows from synaptic depression and reintroduction of depressed or inactive inhibitory interneurons, a transition from tonic to clonic phase occurs. In principle, the slowing of the neurons could be caused by synaptic depression of the neurons (Manor and Nadim 2001; Abbott et al. 1997), neurotransmitter depletion, and/or spike rate adaptation of the neurons. In this paper, we will model how synchrony changes with the slowing of the neurons' firing rates, using synaptic depression and a decrease in the current applied to the neuron over the duration of the seizure.

2 Methods

To illustrate the role of firing rate on synchrony, we use computational simulations of a neuronal network model. The conductance based model neurons have a phase resetting (PRC) that is sensitive to synaptic input firing rate, which essentially equates to the amount of current input to a given cell in time. Our model incorporates synaptic depression, which may be a component of the tonic-clonic transition mechanism. In the section on *Neuronal model* we describe how we modify a standard computational model to have a PRC which is sensitive to firing rate and is similar to those we measure from real neurons. In the section *Pulse coupled oscillator theory*, we describe how to determine if a reciprocally coupled two-cell network will synchronize given the PRC of one neuron, which is then applied to our larger network of neurons as a prediction of population synchrony. Finally, networks that synchronize very quickly are unable show significant changes in synchrony as a function of firing rate. In our simulation we choose a network topology that is able to synchronize or desynchronize, depending on the individual cellular responses. The specific structure of our network is selected and explained from recently published results.

2.1 Neuronal model

We model the neurons using a modified version of the Morris-Lecar (M-L) model (Izhikevich 2007; Morris and Lecar 1981). We choose the M-L model because it is a

reduced Hodgkin-Huxley model (Rinzel 1985) with only two dimensions, so it can be easily analyzed. We find that the dynamics of the M-L model are easily changed by selecting individual parameters within the model. The M-L model has advantages over the Integrate and Fire, quadratic Integrate and Fire, and Izhikevich models in that the PRC of the M-L cell can be made to look similar to PRCs measured from real neurons.

The conductance based M-L model calculates the change in voltage as a function of the membrane ionic currents as described by the following equations:

$$C \dot{V} = I_{input} + I_{noise} - g_L(V - E_L) - g_{Na}m_{\infty}(V)(V - E_{Na}) - g_Kn(V - E_K) - D(S - F)(V - E_{syn}),$$

$$\dot{n} = \frac{n_{\infty}(V) - n}{\tau(V)}$$

$$m_{\infty}(V) = \frac{1}{1 + e^{\frac{V_{1/2} - V}{k}}}$$

$$\tau(V) = C e^{\frac{-(V_{max} - V)^2}{\sigma^2}}$$

$$\dot{S} = -\frac{S}{\tau_s}$$

$$\dot{F} = -\frac{F}{\tau_f}$$

where C is the membrane capacitance, V is the membrane voltage, I_{input} is an input current common to all neurons, I_{noise} is a white noise input proportional to the square root of the time step independent to each neuron, g are the maximal conductances of each current source, E are the reversal potentials for each ion, m and n are the ionic gating variables, where m_{∞} and n_{∞} are the steady-state activation for a given voltage, $V_{1/2m}$ satisfies $m_{\infty}(V_{1/2}) = 0.5$, V_{max} is the value of V at the maximum value of m , k is the degree of slope at $V_{1/2}$, τ is the voltage dependent time constant of the K^+ activation variable, σ determines the sensitivity of the time constant of V , S represents the slow variable of the synaptic input shape, with a time constant τ_s and F is the fast synaptic time constant. At times of synaptic input, 1 is added to both the S and F state variables and depression, D , is defined as $D_{i+1,j} = D_{i,j}d$, updated for cell j after a

synaptic input i as described in (Varela et al. 1997) where the strength of depression is modified by d , set to 0.7 for the simulation.

Our model diverges from the original Morris-Lecar model, which used calcium rather than sodium, but is essentially the same framework. We have also adjusted the parameters so that the PRC is similar to a real neuron's PRC; they are as follows: $C = 1.0 \mu\text{F}$, $g_L = 8 \text{ nS}$, $E_L = -53.24 \text{ mV}$, $g_{\text{Na}} = 18.22 \text{ nS}$, $E_{\text{Na}} = 60 \text{ mV}$, $g_K = 4 \text{ nS}$, $E_K = -95.52 \text{ mV}$, $V_{1/2m} = -7.37 \text{ mV}$, $k_m = 11.97 \text{ mV}$, $V_{1/2n} = -16.35 \text{ mV}$, $k_n = 4.21 \text{ mV}$, $\tau = 1 \text{ ms}$, $\text{spikeWidth} = 0.03$, $E_{\text{syn}} = 0$, $\tau_f = 0.25 \text{ ms}$, $\tau_s = 0.5 \text{ ms}$. We used the minimum changes necessary to produce the dynamics of interest in this paper. A description of how the variables were selected is explained in the results section. Matlab code for this model is available at <http://neuralnetoff.umn.edu/public/TonicClonic> and from Model DB website (<http://senselab.med.yale.edu/modeldb>), an online location for storing and retrieving computational neuroscience models.

2.2 Generating a model PRC

Phase-response curves are directly measured by numerically integrating the model neuron with synaptic inputs at different phases (we used variable time step integrator, ode23 from Matlab (Mathworks)). Current is input into the model oscillator to produce periodic oscillations at a frequency of about 100 Hz. To measure a PRC, a synaptic conductance stimulus is added to the constant current (by setting the state variables S and F to turn on the synaptic conductance waveform) and the resulting change in period is recorded. This is repeated while applying the perturbative stimulus at different phases. The PRC is computed by comparing the perturbed period to the relaxed period at each stimulated point in the phase.

2.3 Pulse coupled oscillator theory

To study how synchrony depends on neuronal firing rate, we use pulse-coupled oscillator theory. Synchrony in a pair of coupled neurons can be predicted from the PRC (Ermentrout and Kopell 1998). If PRCs of two reciprocally coupled neurons are known then it is possible to predict whether they will synchronize by summing the spike-time advance from the synaptic inputs from each neuron onto the other, as shown in Fig. 2. The spike difference from one cycle to the next can be predicted as: $\Delta_{i+1} \approx \Delta_i + PRC_1(\Delta_i) - PRC_2(T - \Delta_i - PRC_1(\Delta_i))$, where Δ_i is the difference in the spike-times of the two neurons on spike i , T is the unperturbed period of two neurons, and $PRC(\Delta)$ determines the change in spike timing of the neurons given a synaptic input at phase Δ .

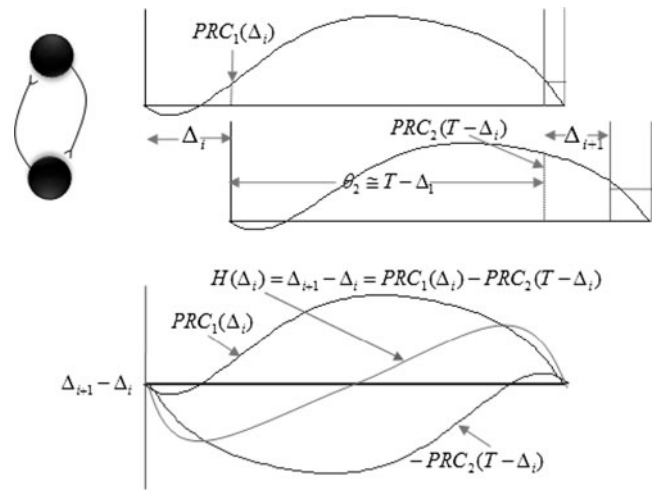


Fig. 2 Illustration of how PRCs can predict changes in spike-time differences on a subsequent cycle. Top: Two reciprocally coupled neurons start at spiketime difference Δ_i . Furthest vertical gray lines show later time T where neurons would fire again if unperturbed. When the bottom cell fires, its synaptic input updates the top cell's firing time according to the top cell's PRC making it actually fire at the penultimate vertical line, and vice-versa for cell 2. These neurons are synchronizing because the time between the two black lines is less than the time between the original two spikes. Bottom: Synchronization can be predicted analytically with the H-function (indicated with arrow), calculated by subtracting PRC_2 reversed in time from PRC_1 . The location of the stable synchronous solution is where the H-function negatively crosses the horizontal phase axis (roots with negative local slope). In this case it occurs at zero phase difference

We simplify the spike difference map for weak coupling by dropping the phase advance argument of PRC_1 in the PRC_2 to

$$\Delta_{i+1} \approx \Delta_i + PRC_1(\Delta_i) - PRC_2(T - \Delta_i).$$

If we linearize the above expression about a zero time lag, we obtain

$$\Delta_{i+1} = \Delta_i + PRC_1(0) + \Delta_i PRC_1'(0) - PRC_2(T) + \Delta_i PRC_2'(T)$$

where the prime indicates the slope. When at synchrony, $PRC_1(0) = PRC_2(T)$, so we simplify to

$$\Delta_{i+1} = \Delta_i(1 + PRC_1'(0) + PRC_2'(T)).$$

The multiplier on the right must have an absolute value less than one for Δ to go to zero. This change in the spike difference between the two neurons from one cycle to the next is called the H -function: $H(\Delta_i) \equiv \Delta_{i+1} - \Delta_i \approx PRC_1(\Delta_i) - PRC_2(T - \Delta_i)$. If the H -function is zero then the spike-time difference is not changing, i.e. $\Delta_{i+1} = \Delta_i$, and the network is at a fixed point in phase. This result is valid under the weak coupling assumption and has been used in our analysis. However, the result under strong coupling has been worked out previously as well (Dror et al. 1999).

For networks of two identical cells with phase resetting constraints at the beginning and end of the phase, one of the fixed points is always at zero-phase (synchronous solution). However, whether or not the system will approach synchrony depends on the stability of the fixed point, which is determined by the slope of the H -function at that point. When evaluating the synchronous state, the slope of the H -function must be $-1 < PRC'_1(0) + PRC'_2(T) < 0$ for synchrony to be stable. According to Achuthan and Canavier, the slope of the H -function is the eigenvalue of the system and thus the rate of convergence to synchrony is dependent on that eigenvalue (Achuthan and Canavier 2009). The steeper (i.e. more negative) the slope of H -function is at zero-phase, the faster the network will synchronize and the tighter the two cells will stay in synchrony in the presence of noise. It is appropriate to extend this theory to a larger network, provided the inputs of the network to a given cell do not push the H -function outside of the stability range.

3 Network simulations

Networks of 3000 M-L neurons were directionally connected with an average of 30 out-going excitatory synaptic connections each. The neurons were started in “splay phase” with initial phases evenly distributed around the limit cycle. Current was applied to all neurons as well as a small independent white noise input, representing intrinsic noise and unshared synaptic inputs from other brain areas. The noise was used to create variability in the cellular firing rates to produce a non-deterministic system. The network was modeled as a homogeneous population of excitatory neurons assuming the inhibitory population has failed, resulting in runaway excitation. Over the simulation duration, the nominal current is ramped down to represent the gradual reintroduction of the inhibitory population until the action potentials cease.

3.1 Network structure

Networks were generated using a second order network model framework (Zhao et al. 2011), which allows additional correlated structure to random networks. The specific network structure is determined by specifying the average connectivity (first order statistic) as well as the prevalence of combinations of pairs of connections (two edges), called second order motifs. These second order motifs are reciprocal connections, convergent connections, divergent connections, and chain connections, as illustrated in Fig. 3. Using the second order network framework, one can specify the frequency of these second order motifs (relative to a model where all connections are generated

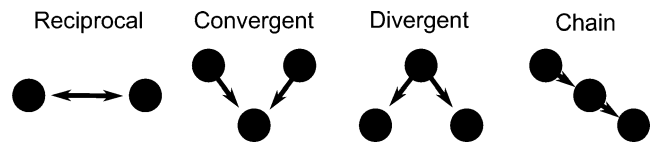


Fig. 3 Second order motifs of two and three-cell combinations with two directional connections. The motifs are reciprocal, convergent, divergent, and chain motifs. The prevalence of these motifs within a larger network can be specified when generating the network

independently) and generate large networks containing the specified proportions of these motifs. For example, the parameter of 1.4 for the convergent motif means that there are 1.4 times as many convergent connections in the generated network compared to a random network. The prevalence of each motif can drastically change the synchronizability of the network, which we will discuss further.

3.2 Measuring synchrony with the Kuramoto order parameter

Ultimately the tonic-clonic seizure dynamics are a population phenomenon. The application of a model neuron into a network of similar model neurons becomes an important test to compare our model to recorded neural network data during a tonic-clonic seizure. To quantify the changing synchrony in the network, we use the Kuramoto order parameter defined as follows,

$$r e^{i\phi} = \frac{1}{N} \sum_{j=1}^N e^{i\theta_j}$$

where N is the number of cells in the simulation, θ_j is the phase of the j^{th} oscillator, ϕ is the group phase, and r is the phase coherence of the ensemble of oscillators (Strogatz 2000). Synchrony is determined by the length of the population vector, r . This vector is calculated by summing the individual phase vectors of all neurons, which is normalized to 1 by the total number of cells N . A value of $r=1$ represents a full coherent synchrony of the ensemble, while a value of $r=0$ represents an ensemble of oscillators evenly distributed in phase. We compute the Kuramoto order parameter throughout the simulation to study how the coherence of the network changes in time.

4 Results

4.1 PRCs measured from Morris-Lecar model

Phase-response curves from Morris-Lecar (M-L) model neurons are generated using the direct method of applying synaptic input and measuring the change in firing time, as shown in Fig. 2. Our goal is to use a model where the shape

of the PRC changes with firing rate and to tune the model to generate a PRC similar to those measured from real neurons (Netoff et al. 2005). Since the PRC changes with input, it is important to understand how those changes can predict the synchrony of a network. When measuring PRCs from the M-L model, we compare them to those measured in real cells. An example of an experimentally measured PRC is shown in Fig. 4. Here, the PRC has been measured with synaptic-like (alpha function) perturbations which are strong compared to the expected strength of an individual synaptic input. This is important when considering the seizure model where many inputs may be arriving at a cell within a firing cycle, especially in the bursting clonic phase where large coherent signals are present. To tune the M-L model accordingly, we used phase plane analysis and selected parameters that produced a more realistic PRC.

The dynamics of the M-L model can be determined graphically from the state plane representation, where we plot the voltage (V) against the activation value (n), as shown in Fig. 5. The nullclines are plotted, and crossings of the nullclines are fixedpoints, which may be stable or unstable. When one unstable fixedpoint exits, the neuron fires periodically making a closed loop path, known as a limit cycle, and can be seen as the dotted loop in Fig. 5. If an input to the neuron perturbs it from the limit cycle, it will relax back to this periodic path.

The phase response curve determines how a stimulus phase advances the neuron. This can be seen graphically by plotting the isochrones in the state space. Isochrones are lines in state space of the model where all the points

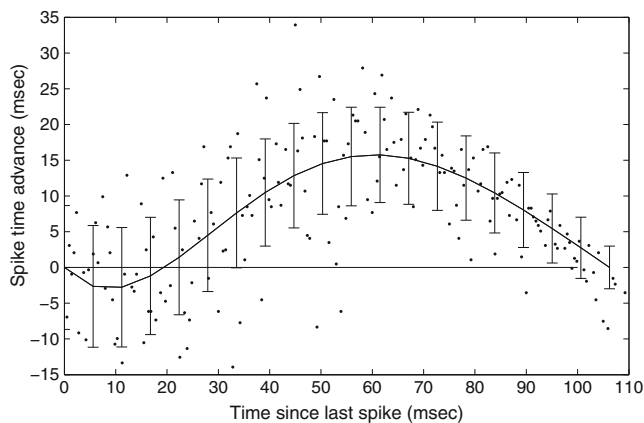


Fig. 4 Phase-response curve measured from an excitatory pyramidal cell in the hippocampal region using dynamic patch clamp. Dots are experimental measurements of individual perturbations. Data is fit using a 5th order polynomial which is constrained to zero-spike-time advance at zero-phase and similarly constrained at the end of the neuron's phase. The period of this cell is about 107 ms. Positive values represent an advance of the next neuronal spike (decreasing the period) and negative values represent a delay of the next spike (increasing the period). The spike-time advance variability, shown as uncertainty bars, is smaller in the later parts of the neuron's phase. There is a horizontal axis line for reference

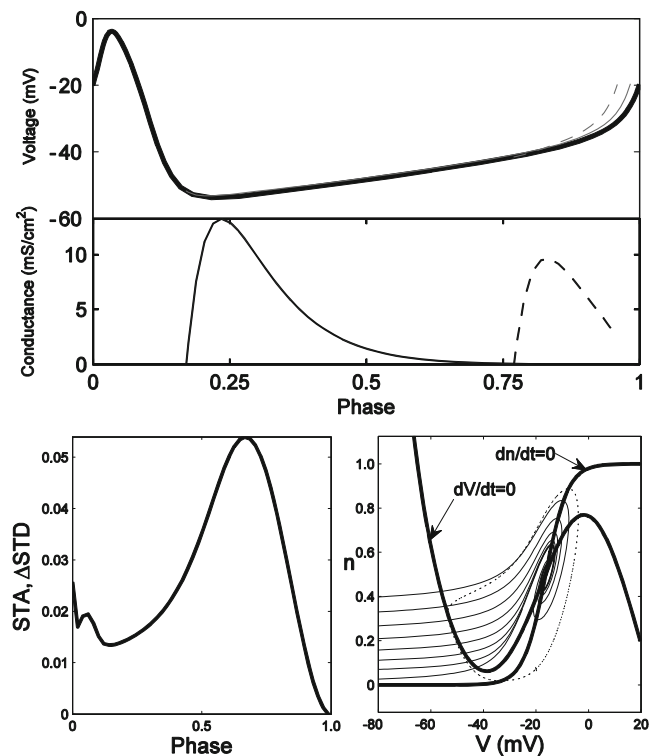


Fig. 5 Top: Voltage trace of the modified Morris-Lecar model for one cycle. Thick line is the model with no input, thin line and dotted line for synaptic inputs applied at different phases, as indicated by the conductance below. Bottom Left: Measured PRC. Bottom Right: Nullclines (thick lines), limit cycle (dotted) and isochrones (thin lines)

converge to the same phase of the limit cycle (Izhikevich 2007). If the stimulus cuts across dense lines of isochrones, there will be a large change in phase, while if the stimulus pushes the neuron along isochrones the phase will not change. Synaptic inputs generate current and move the V -isocline up temporarily, which causes the limit cycle to move and the states of the neurons to cut across the isochrones. To make the PRCs of the M-L neuron have the shape similar to PRCs measured from real neurons, we changed the parameters of the model so that the resulting isochrones intersected the limit cycle at oblique angles. As the V -nullcline is moved up and down, the intersection of the isochrones with the limit cycle changed significantly, resulting in changes in the shape of the PRC. Animations of the isochrones as a function of input current can be seen at <http://neuralnetoff.umn.edu/public/TonicClonic>.

4.2 PRCs as a function of input current

As the firing rate of a neuron increases, the PRC changes in shape and amplitude. In the M-L model, the PRC amplitude decreases as the firing rate increases. This indicates that at high firing rates a synaptic input would cause less phase advance than would occur at the same phase at a lower firing rate, as shown in Fig. 6. At high firing rates the

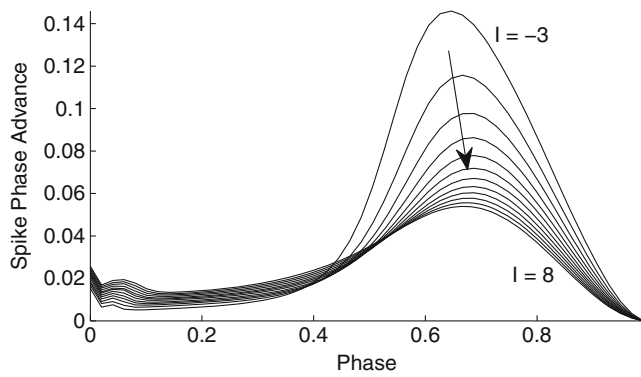


Fig. 6 Phase-response curves as a function of firing rate. As the current input to the model is increased from -3 nA to 8 nA, the PRC amplitude decreases

neuron becomes dominated by its own internal dynamics and is less influenced by external inputs.

4.3 Network synchrony as a function of current as predicted by H-function

The synchronizability of a reciprocally connected two-cell network can be predicted from each cell’s PRC by analyzing the slope of the H -function at the in-phase solution (Neu 1979). Figure 7 shows the H -function and the slope at the zero-phase for a range of firing rates of the M-L model. The slope is most negative around the synchronous solution for lower input currents, indicating that synchrony is more strongly attracting as long as the slope of the H -function remains between 0 and -1 (Achuthan and Canavier 2009). As the current increases, the magnitude of the slope decreases, thus, the synchrony becomes less attracting. The slope of the zero-phase solution remains negative, indicating

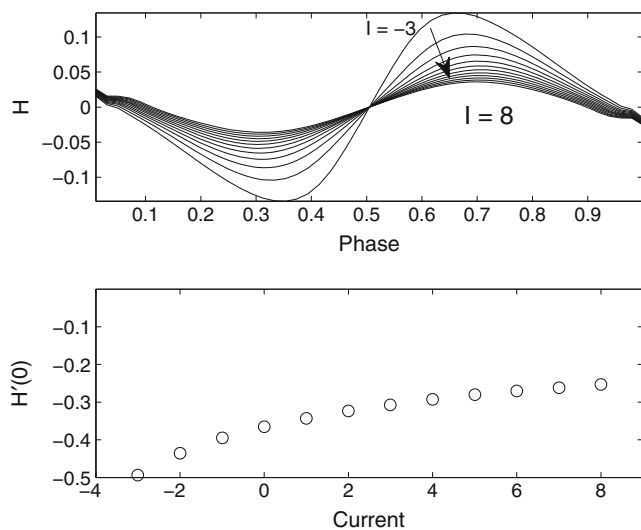


Fig. 7 Top: H -function of M-L model for a range of firing rates modeled as current input. Bottom: Slope of H -function at zero-phase increases for increasing current

that network synchrony remains stable, as discussed in Goel and Ermentrout (Goel and Ermentrout 2002). The H -function predicts synchrony in a two cell network, therefore we generated large scale networks to determine if these predictions are valid when network size is increased.

4.4 Seizure simulation

At the onset of the tonic phase, neurons are firing more frequently than normal (Ward 1961). If the inhibitory population is no longer firing, the excitatory population fires uncontrolled at high rates. As the excitatory neurons fatigue or synaptically accommodate (or through some other unknown mechanism), the firing rate decreases and thus the input to individual cells decreases. To model this biological process, we begin our simulation at high external input current and end at a lower external input current.

We simulate a network of M-L neurons directionally coupled using a second order network topology which has 4 times the number of reciprocal connections, 1.4 times the number of convergent connections, 1.3 times the number of divergent connections and 1.2 times the number of chain connections than would be expected from a randomly generated network. Over the duration of the simulation, the current injected into each cell was decreased from $I=8$ nA, where the neurons fired at high rates (6 ms period or interspike interval (ISI)) to $I=-3$ nA, where they fired less frequently. Initialized in splay phase, synchrony was initially low with high current and as the current input was decreased, the firing rate diminished and the network synchrony increased, illustrated in Fig. 8. This simulation

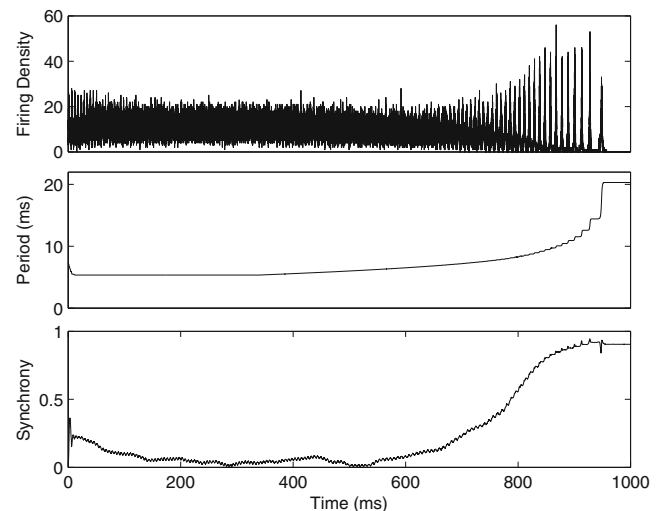


Fig. 8 Synchrony in large scale networks. A network simulation of 3000 Morris-Lecar model neurons using second order network topology. Current applied to neurons starts at 8 nA and decreases to -4 nA over the duration of the simulation. Top, firing density, the number of neurons firing in 1 ms window. Middle, ISI of average neuron in network. Bottom, the Kuramoto order parameter measuring network synchrony

demonstrates how a seizure may transition from an asynchronous tonic phase to a synchronous clonic phase with the change in current drive to individual cells. Figure 8 shows that early in the simulated seizure, the neurons are firing at a high density of asynchronous firing (dense low amplitude values in top panel) with high frequency (small interspike intervals in middle panel) and a low degree of synchrony (bottom panel). As the current input is decreased, the firing rates of the neurons decrease (increasing the ISI) and the synchronous solution is more strongly attracting, resulting in low frequency and high amplitude oscillations in the population density. The synchrony is high until the input current falls below the firing threshold (into resting stability) of the neurons and the system stops activity.

To assure that the initial conditions are not responsible for the asynchrony during the first section of the simulation (with high current input), we initialize simulations in a synchronous state. These simulations desynchronize initially (not shown) with high current input. Thus we conclude the asynchronous behavior at the beginning of the simulation cannot be solely attributed to the initial conditions. In longer simulations where the current is ramped more slowly, the transition to synchrony occurs more gradually, indicating the change in synchrony is determined by a change in the strength of the synchronous state (due to the current input) and not due to transients.

When including synaptic depression, the high frequency of neuron firing at the beginning of the seizure depresses the synaptic input and thus decreases the strength of subsequent synaptic events. This model also produces the tonic-clonic transition over a smaller range of input current at lower values as shown in Fig. 9. The experiment demonstrates that a combination of synaptic depression and an increasing negative current (from inhibitory neurons being released from depolarization block) may be responsible for the shift in synchrony.

4.5 Network topology role in synchrony

Neuronal topology played a critical role in how strongly the network synchronized. In M-L networks with random connections or complete connections (all-to-all coupling), synchrony was strong at all firing rates. We then connected the neurons in a small-world network (Watts and Strogatz 1998), where a ring of neurons has local connections, some of which are randomly rewired, as we have used in earlier papers (Netoff et al. 2004). While the randomly connected networks synchronize strongly (even with very weak coupling) the small world networks did not synchronize well under any coupling strength. Therefore, it was necessary to create a network which would synchronize strongly with low input and less strongly with high input. Specifically, our network must be sensitive to the current to

individual M-L cells, as that is our variable parameter. In order to have the network simulation produce the tonic-clonic shift, it was necessary to select a network with a more biologically realistic topology.

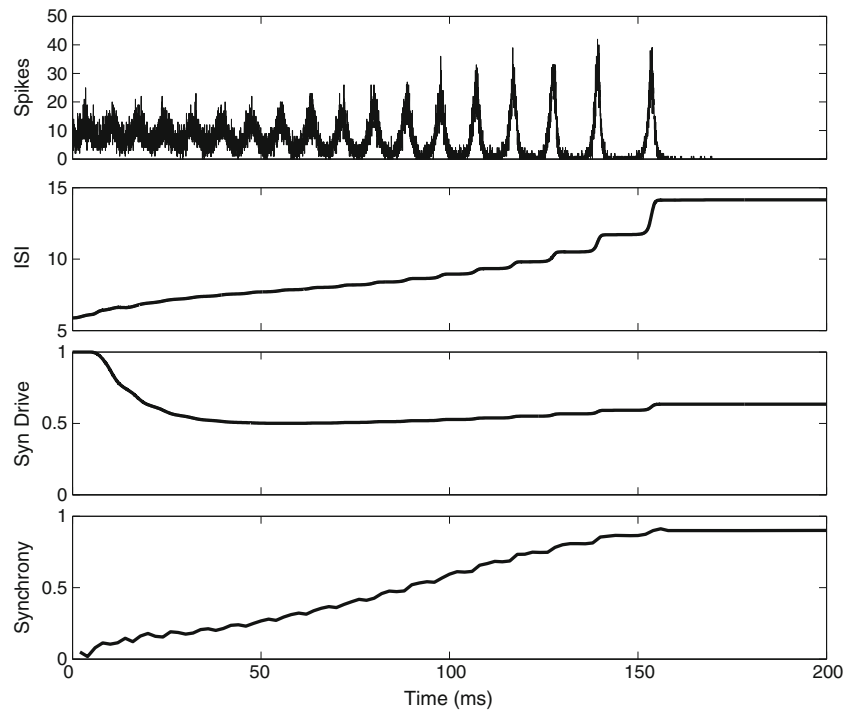
We generated second-order networks (Zhao et al. 2011) to examine the change in synchrony from high input to low input. We found that networks in a certain parameter regime of connectivity changed synchrony as the firing rate of the constituent neurons changed. Thus, networks of second order statistics were able to produce the desired sensitivity of synchrony to input. In Fig. 10 we plot the level of synchrony in color against the prevalence of chains and convergent motifs (compared to a random network) of 186 SONETs for neurons. The cells were driven with high current (left), low current (middle), and current ramped from high to low, plotted as the difference in synchrony extrema. Using these results we were able to choose a specific network to conduct our simulation of the tonic-clonic transition. The network topology used in Fig. 8 was chosen with second-order motif construction. The specific network topology (we refer to as 4432) was also very close to the statistics of experimentally measured multi-cell motifs in rat cortex from Song et al. (Song et al. 2005). We believe this network is an example of a realistic network topology where the transition from tonic-clonic caused by change in synchrony can occur as firing rate of the neurons changes.

5 Discussion

During tonic-clonic seizures, network synchrony changes, evidenced from EEG data. We hypothesize that this change in synchrony is caused by changes in the neuronal firing rate. Using computational models, we demonstrate using PRC analysis that the attraction of synchrony in a two-cell network changes with firing rate of the neurons. The analysis revealed that the synchronous network solution was not as stable at high current (high firing rates) compared to low current, suggesting that the tonic phase was the result of a high current input system and the more synchronous clonic phase was the result of a low current input system. Using network simulations with decreasing input current to the neurons and/or synaptic depression, we were able to simulate the change in network synchrony and qualitatively reproduce the tonic-clonic shift.

To reproduce the tonic to clonic transition in a model, it was necessary to use cells whose sensitivity to synaptic inputs were dependent on the firing rate of the neurons and a network topology that allowed for synchrony, but was not so strongly connected that synchrony was inevitable under all coupling strengths. Therefore we tuned our neuronal model to produce realistic looking PRCs across a range of

Fig. 9 Synchrony in large scale networks with synaptic depression. Same network statistics as Fig. 8 with current range from $I=0$ nA to $I=-5$ nA and inclusion of synaptic depression. Average synaptic strength in time as plotted in 3rd panel as Synaptic Drive. Note duration of this simulation is less than in previous network



input currents to achieve the first requirement. Previous studies have shown that network topology can have a major effect on the synchronizability of a PRC network (Smeal et al. 2010). To fulfill our second necessary condition of a range of synchrony and biological relevance, we used a specific second-order network topology (SONET) which was able to synchronize at low input current and

desynchronize at high input current. The choice of topology 4432 was motivated by an inquiry into the synchronizability of 186 SONETs for different currents and the similarity of the 4432 network to experimentally measured cortical brain tissue.

The network simulations were run with a simple conductance based model neuron, the Morris-Lecar model. By

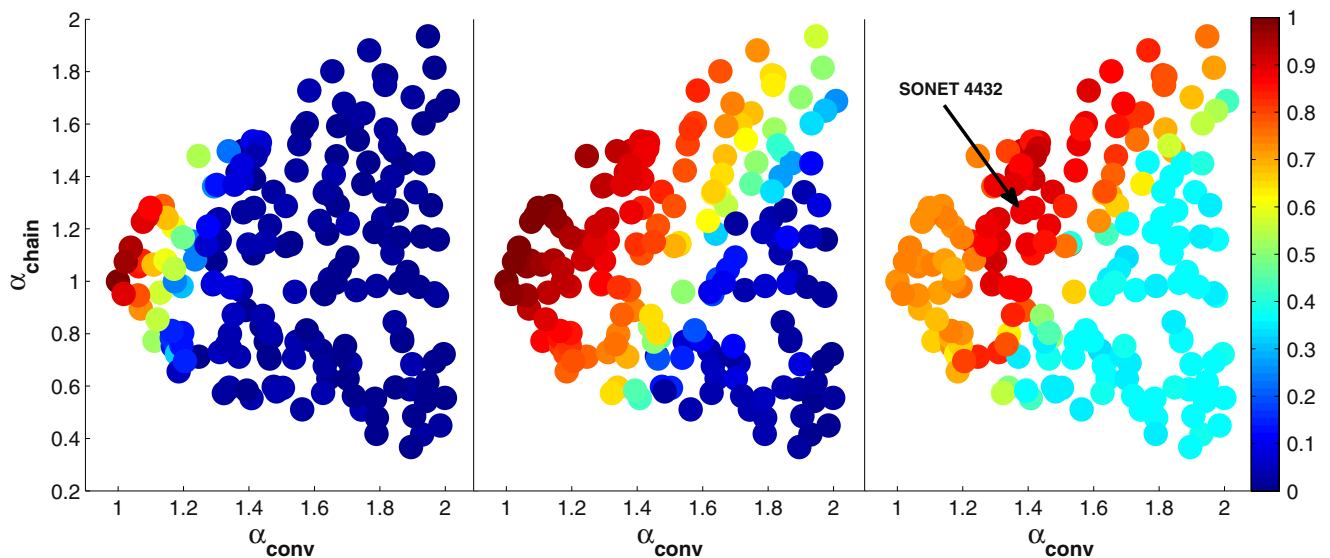


Fig. 10 Second Order networks. Degree of synchrony (color) of M-L network simulations for a range of second order network topologies (SONETs). The networks are characterized by the prevalence of two-edge motifs (here chain and convergent) compared to a random topology. Left, High input current $I=7$ nA. Middle, Low input current $I=-2$ nA. Right, Difference of synchrony at the beginning and end of

network simulation from ramping current from high to low. In Right, Red points indicate there is a large difference in synchrony from beginning to end of simulation, which is where we select our specific network (SONET 4432) to model the tonic-clonic transition, indicated with arrow

adjusting the model parameters, we were able to create a PRC with moderate phase advance throughout the entire phase and a larger peak. The M-L model generated PRCs that were similar to those we have measured from real neurons and these PRC shapes were dependent on the external current. In the M-L model, as the firing rate decreased, the amplitude of the PRC increased but the shape generally did not change. Thus, the PRC amplitude effectively changed the functional coupling between the cells.

It is known from coupled oscillator theory that there is a critical coupling strength necessary to synchronize neurons in the presence of noise (Strogatz 2000; Kuramoto 1984). Our networks of neurons coupled with all-to-all or random topology synchronized under both fast and slow firing rates, indicating the effective coupling in both conditions was greater than the critical coupling strength for synchrony. Changing topology of the network can affect the critical coupling strength required for the network to synchronize (Zhao et al. 2011). We chose a second-order network topology such that the functional coupling for the neurons at the highest firing rate was below the critical coupling and above the critical coupling at the lower firing rate. This selection of topology allowed for the network to transition from asynchrony to synchrony as neurons changed firing rate.

Previous studies have examined the dependence of synchrony on firing rate (Mancilla et al. 2007; Tiesinga and Sejnowski 2004; Buia and Tiesinga 2006; Fink et al. 2011). Changes in firing rate have been used to explain the emergence and disappearance of gamma oscillations in coupled networks (Mancilla et al. 2007). Fink et al. have shown that synchrony is affected more by firing rate in networks of Type II PRC models than Type I models with small-world network topology (Fink et al. 2011). While our modeling did not result in extreme change from Type I to Type II (ours were only Type I), our results are in concordance with their findings.

6 Conclusion

Network simulations using Morris-Lecar models coupled with a second order network topology increased synchrony as the firing rates of the neurons decreased. This model illustrates a possible mechanism by which grand-mal seizures may transition from the tonic to clonic phase. The network simulations were modeled using a homogeneous population of excitatory cells under the hypothesis that the seizure was initiated by the failure of the inhibitory population, allowing runaway excitation. The firing rates of the neurons were changed by adjusting the applied current and also including synaptic depression to isolate a single factor, the average network firing rate, illustrating how

synchrony can change with the phase response of the individual neurons. Realistically, the change in firing rate is determined by several factors including the firing rate of the pre-synaptic neurons. The post-synaptic neurons may slow their firing rate as they adapt to strong synaptic drive and these synapses may depress under high firing rate (Abbott et al. 1997). The combination of the two may result in a decrease of the firing rate of the neurons over the course of the seizure inducing a bifurcation in population synchrony.

Acknowledgments Thanks to Bard Ermentrout and Chris Warren for helpful discussions. Funding for this work provided by UMN Grant-In-Aid and NSF CAREER award.

References

- Abbott, L. F., Varela, J. A., Sen, K., & Nelson, S. B. (1997). Synaptic depression and cortical gain control [see comments]. *Science*, 275(5297), 220–224.
- Achuthan, S., & Canavier, C. C. (2009). Phase-resetting curves determine synchronization, phase locking, and clustering in networks of neural oscillators. *The Journal of Neuroscience: The Official Journal of the Society for Neuroscience*, 29(16), 5218–5233.
- Bragin, A., Engel, J., Jr., & Staba, R. J. (2010). High-frequency oscillations in epileptic brain. *Current Opinion in Neurology*, 23(2), 151–156.
- Brown, E., Moehlis, J., & Holmes, P. (2004). On the phase reduction and response dynamics of neural oscillator populations. *Neural Computation*, 16(4), 673–715.
- Buia, C., & Tiesinga, P. (2006). Attentional modulation of firing rate and synchrony in a model cortical network. *Journal of Computational Neuroscience*, 20(3), 247–264.
- Dror, R. O., Canavier, C. C., Butera, R. J., Clark, J. W., & Byrne, J. H. (1999). A mathematical criterion based on phase response curves for stability in a ring of coupled oscillators. *Biological Cybernetics*, 80(1), 11–23.
- Ermentrout, G. B., & Kleinfeld, D. (2001). Traveling electrical waves in cortex: insights from phase dynamics and speculation on a computational role. *Neuron*, 29(1), 33–44.
- Ermentrout, G. B., & Kopell, N. (1998). Fine structure of neural spiking and synchronization in the presence of conduction delays. *Proc Natl Acad Sci U S A*, 95(3), 1259–164.
- Ermentrout, G. B., Beverlin, B. 2nd, Troyer, T., & Netoff, T. I. (2011). The variance of phase-resetting curves. *Journal of Computational Neuroscience*
- Fink, C. G., Booth, V., & Zochowski, M. (2011). Cellularly-driven differences in network synchronization propensity are differentially modulated by firing frequency. *PLoS Computational Biology*, 7(5), e1002062.
- Fisch, J. F., & Olejniczak, P. W. (2006). Generalized-tonic-clonic seizures. In E. Wyllie, A. Gupta, & D. K. Lachhwani (Eds.), *The treatment of epilepsy: Principles & practice* (p. 279). Philadelphia: Lippincott Williams & Wilkins.
- Garcia Dominguez, L., Wennberg, R. A., Gaetz, W., Cheyne, D., Snead, O. C., 3rd, & Perez Velazquez, J. L. (2005). Enhanced synchrony in epileptiform activity? local versus distant phase synchronization in generalized seizures. *The Journal of Neuroscience: The Official Journal of the Society for Neuroscience*, 25(35), 8077–8084.
- Gastaut, H., & Broughton, R. J. (1972). *Epileptic seizures: clinical and electrographic features, diagnosis and treatment*. Springfield: Thomas.

- Glass, L., & Mackey, M. C. (1988). *From clocks to chaos: The rhythms of life*. Princeton: Princeton University Press.
- Goel, P., & Ermentrout, G. B. (2002). Synchrony, stability, and firing patterns in pulse-coupled oscillators. *Physica D: Nonlinear Phenomena*, 163(3–4), 191.
- Hansel, D., Mato, G., & Meunier, C. (1995). Synchrony in excitatory neural networks. *Neural Comput*, 7(2), 307–37.
- Hoppensteadt, F. C., & Izhikevich, E. M. (1997). *Weakly connected neural networks*. New York: Springer.
- Izhikevich, E. M. (2007). *Dynamical systems in neuroscience: The geometry of excitability and bursting*. Cambridge: MIT.
- Kopell, N., & Ermentrout, G. B. (2002). Mechanisms of phase-locking and frequency control in pairs of coupled neural oscillators. In B. Fiedler (Ed.), *Handbook on dynamical systems* (pp. 3–54). New York: Elsevier.
- Kuramoto, Y. (1984). *Chemical oscillations, waves, and turbulence*. Berlin: Springer.
- Lewis, T. J., & Rinzel, J. (2003). Dynamics of spiking neurons connected by both inhibitory and electrical coupling. *Journal of Computational Neuroscience*, 14(3), 283–309.
- Mancilla, J. G., Lewis, T. J., Pinto, D. J., Rinzel, J., & Connors, B. W. (2007). Synchronization of electrically coupled pairs of inhibitory interneurons in neocortex. *The Journal of Neuroscience: The Official Journal of the Society for Neuroscience*, 27(8), 2058–2073.
- Manor, Y., & Nadim, F. (2001). Synaptic depression mediates bistability in neuronal networks with recurrent inhibitory connectivity. *J Neurosci*, 21(23), 9460–9470.
- Morris, C., & Lecar, H. (1981). Voltage oscillations in the barnacle giant muscle fiber. *Biophysical Journal*, 35(1), 193–213.
- Neltner, L., Hansel, D., Mato, G., & Meunier, C. (2000). Synchrony in heterogeneous networks of spiking neurons. *Neural Comput*, 12(7), 1607–41.
- Netoff, T. I., & Schiff, S. J. (2002). Decreased neuronal synchronization during experimental seizures. *The Journal of Neuroscience: The Official Journal of the Society for Neuroscience*, 22(16), 7297–7307.
- Netoff, T. I., Clewley, R., Arno, S., Keck, T., & White, J. A. (2004). Epilepsy in small-world networks. *The Journal of Neuroscience: The Official Journal of the Society for Neuroscience*, 24(37), 8075–8083.
- Netoff, T. I., et al. (2005). Synchronization in hybrid neuronal networks of the hippocampal formation. *Journal of Neurophysiology*, 93(3), 1197–1208.
- Neu, J. (1979). Coupled chemical oscillators. *SIAM J. Appl. Math.*, 37(307–315).
- Perez Velazquez, J. L., Garcia Dominguez, L., & Wennberg, R. (2007). Complex phase synchronization in epileptic seizures: Evidence for a devil's staircase. *Physical Review E, Statistical, Nonlinear, and Soft Matter Physics*, 75(1 Pt 1), 011922.
- Quiñero, R., Blanco, S., Rosso, O. A., Garcia, H., & Rabinowicz, A. (1997). Searching for hidden information with gabor transform in generalized tonic-clonic seizures. *Electroencephalography and Clinical Neurophysiology*, 103(4), 434–439.
- Rinzel, J. (1985). Excitation dynamics: Insights from simplified membrane models. *Federation Proceedings*, 44(15), 2944–2946.
- Schindler, K., Elger, C. E., & Lehnertz, K. (2007). Increasing synchronization may promote seizure termination: evidence from status epilepticus. *Clinical Neurophysiology: Official Journal of the International Federation of Clinical Neurophysiology*, 118(9), 1955–1968.
- Schindler, K., Leung, H., Elger, C. E., & Lehnertz, K. (2007). Assessing seizure dynamics by analysing the correlation structure of multichannel intracranial EEG. *Brain: A Journal of Neurology*, 130(Pt 1), 65–77.
- Smeal, R. M., Ermentrout, G. B., & White, J. A. (2010). Phase-response curves and synchronized neural networks. *Philosophical Transactions of the Royal Society of London. Series B, Biological Sciences*, 365(1551), 2407–2422.
- Song, S., Sjöström, P. J., Reigl, M., Nelson, S., & Chklovskii, D. B. (2005). Highly nonrandom features of synaptic connectivity in local cortical circuits. *PLoS Biology*, 3(3), e68.
- Strogatz, S. H. (2000). From Kuramoto to Crawford: exploring the onset of synchronization in populations of coupled oscillators. *Physica D: Nonlinear Phenomena*, 143(1–4), 1.
- Tiesinga, P. H., & Sejnowski, T. J. (2004). Rapid temporal modulation of synchrony by competition in cortical interneuron networks. *Neural Computation*, 16(2), 251–275.
- Varela, J. A., Sen, K., Gibson, J., Fost, J., Abbott, L. F., & Nelson, S. B. (1997). A quantitative description of short-term plasticity at excitatory synapses in layer 2/3 of rat primary visual cortex. *J Neurosci*, 17(20), 7926–740.
- Ward, A. A. Jr. (1961). The epileptic neurone. *Epilepsia*, 270–280.
- Watts, D. J., & Strogatz, S. H. (1998). Collective dynamics of 'small-world' networks. *Nature*, 393(6684), 440–442.
- Winfree, A. T. (2001). *The geometry of biological time*. New York: Springer.
- Zhao, L., Beverlin B. 2nd, Netoff, T., & Nykamp D. Q. (2011). Synchronization from second order network connectivity statistics. *Frontiers in Computational Neuroscience*, 528.
- Ziburkus, J., Cressman, J. R., Barreto, E., & Schiff, S. J. (2006). Interneuron and pyramidal cell interplay during *in vitro* seizure-like events. *Journal of Neurophysiology*, 95(6), 3948–3954.